A neural-counting model incorporating refractoriness and spread of excitation. I. Application to intensity discrimination

Malvin Carl Teich and Gerard Lachs[a)]

Columbia University, Department of Electrical Engineering, New York, New York 10027
(Received 10 August 1978; accepted for publication 23 August 1979)

We consider in detail a new mathematical neural-counting model that is remarkably successful in predicting the correct detection law for pure-tone intensity discrimination, while leaving Weber's law intact for other commonly encountered stimuli. It incorporates, in rather simple form, two well-known effects that become more marked in the peripheral auditory system as stimulus intensity is increased: (1) the spread of excitation along the basilar membrane arising from the tuned-filter characteristics of individual primary afferent fibers and (2) the saturation of neural counts due to refractoriness. For sufficiently high values of intensity, the slope of the intensity-discrimination curve is calculated from a simplified (crude saturation) model to be $1-1/4N$, where N is the number of poles associated with the tuned-filter characteristic of the individual neural channels. Since $1 \leq N < \infty$, the slope of this curve is bounded by 3/4 and 1 and provides a theoretical basis for the "near miss" to Weber's law.

PACS numbers: 43.66.Ba, 43.66.Fe, 43.66.Lj [DM]

INTRODUCTION

Though the first experiments on pure-tone intensity discrimination in audition were performed by Riesz in 1928, this same topic continues to draw lively interest some 50 years later. Why does this fundamental discrimination problem continue to perplex us, when the seemingly more difficult companion discrimination problems of tone-in-noise, and noise-in-noise, appear to have long ago yielded to solution? The answer, we believe, lies in the substantially greater role that saturation effects play in the pure-tone case.

Indeed, saturation has been increasingly drawn into the picture as a central element in a number of attempts to understand the outcomes of psychophysical discrimination experiments in the past decade. Yet, mathematical models incorporating the effect have, for the most part, been phenomenological in nature. In this work, we specifically link the saturation of counts in individual neural channels with a nonparalyzable *dead-time*[1] process, and, in accord with neurophysiological evidence for individual fibers, ascribe to each channel a tuned-filter characteristic. In essence, therefore, our "discriminating ear" consists of a collection of dead-time-modified, neural-counting channels in the auditory system, a greater and greater number of which respond to the stimulus as the intensity (or energy) of the latter is increased. We thereby provide a *spread-of-excitation* model that is based on neurophysiological data; fortunately, it yields workable expressions for the statistical quantities that we must have in order to perform calculations of discriminability.

There have been a substantial number of experimental measurements relating to pure-tone intensity discrimination over the years. For a sufficiently high intensity baseline, all of the experimental data (gathered over a great variety of stimulus durations and frequencies) are consistent with a straight-line intensity-discrimination curve[2] whose slope measures approximately 9/10 when energy units are used (Riesz, 1928; Churcher, King, and Davies, 1934; Dimmick and Olson, 1941; Harris, 1963; Campbell, 1966; Campbell and Lasky, 1967; Green, 1967; McGill and Goldberg, 1968a, 1968b; Viemeister, 1972; Schacknow and Raab, 1973; Moore and Raab, 1974; Luce and Green, 1974, 1975; Penner *et al.*, 1974; Rabinowitz *et al.*, 1976; Jesteadt, Wier, and Green 1977; Green *et al.*, 1979). In particular, Rabinowitz *et al.* (1976) averaged the intensity-discrimination data from 15 recent studies, all conducted at 1000 Hz, and concluded that the average slope was 0.91 for intensities between 40- and 90-dB sensation level (SL). Since a slope of unity for this curve defines Weber's law, McGill and Goldberg (1968b) referred to the outcome of $\frac{9}{10}$ for the slope as a "near miss" to Weber's law. The phrase has stuck. The near miss indicates that intensity discrimination for the pure-tone case is superior to that for the tone-in-noise and noise-in-noise cases, for which Weber's law has been shown to be satisfied experimentally over virtually the entire range of SL's (Hawkins and Stevens, 1950; Miller, 1947).

It is also of interest to note that Rabinowitz *et al.* (1976) reported that tone-in-tone intensity discrimination obeys Weber's law for SL's at moderate intensities (between 10 and 40 dB), and that a slope shallower than unity (a miss to Weber's law) again obtains for SL's below 10 dB. Our model is also in accord with these observations, and we discuss this region in the final section of the paper.

McGill (1967) has constructed an elegant neural-counting model, based on the mass flow of information in the ear, that yields Weber's law for the tone-in-noise and noise-in-noise cases. It is also not difficult to construct a theoretical model that yields a detection law substantially different from Weber's law. For example,

[a)]Permanent address: The Pennsylvania State University, Department of Electrical Engineering, University Park, PA 16802.

 0001-4966/79/121738-12$00.80

if we form the hypothesis that a brief auditory stimulus creates a simple Poisson neural-counting process with a count rate n directly proportional to the stimulus energy E, we arrive at the deVries–Rose "square-root" detection law (deVries, 1943; Rose, 1942; McGill, 1967, 1971). This law is represented by a straight-line intensity-discrimination curve with a slope of $\frac{1}{2}$. Recognizing this, McGill and Goldberg (1968a, 1968b) retained McGill's earlier assumption of a Poisson neural-counting process (McGill, 1967, 1971) but chose the detected count rate to be proportional to E^p, where $p \sim \frac{1}{5}$ $(0 < p \leq 1)$, rather than to E^1. This interesting saturation device provided a compressed range for the count rate that agreed quite well with neurophysiological measurements over the enormous range of audible stimuli, and at the same time yielded reasonable correspondence with loudness functions. It also provided a straight-line intensity-discrimination curve with a slope of $1 - (p/2)$, which is bounded by the deVries–Rose law and Weber's law, as experiment appears to require. In this model, the quantity p is determined from the data.

In 1972, Penner postulated a modified version of this model in which the (compressed) energy undergoes Poisson transduction independently in a number of channels, with subsequent summation of the resulting neural counts. She referred to this as "neural summation" in contrast to McGill's "energy summation." Extensive neurophysiological measurements on the cat and monkey tell us that indeed individual primary auditory fibers transmit digitally coded neural information, display strong saturation effects, and appear to be statistically independent[3] (Galambos and Davis, 1943; Kiang *et al.*, 1965; Rose *et al.*, 1971; Johnson and Kiang, 1976). Since the VIIIth nerve appears to be the exclusive pathway for the transmission of auditory information to the higher centers of the central nervous system, we also adopt the point of view that intensity discrimination involves the processing of neural counts in multiple channels. A related multiple-channel model was set forth earlier by Siebert (1965), but he did not deal with the near miss to Weber's Law.

In spite of the fact that both the McGill–Goldberg and Penner models are enticing in their simplicity, neither is altogether satisfactory. In the first place, neither McGill and Goldberg nor Penner account for the observed frequency response characteristics of the individual channels, and in the second place, the assumed power-law relationship of count rate to energy has been formed on an *ad hoc* basis. We remedy both of these deficiencies in our model.

Another class of models, on which less analytical work has been carried out, comprises the spread-of-excitation models (Zwicker, 1956, 1970; Schuknecht, 1960; Bos and deBoer, 1966; Whitfield, 1967). The assumption here—and it is based on firm neurophysiological evidence—is that the excitation pattern stimulated by a pure tone will spread out along the basilar membrane as the intensity of the tone is increased. The effect is not small, and we account for it in our model by assuming frequency roll-off characteristics for individual neural channels.

A number of other researchers have constructed detailed neural-counting and neural-timing models based on the statistical data observed from auditory fibers excited by pure-tone stimuli. Luce and Green (1972, 1974, 1975) modeled the successive spike interarrival times (IATs) from first-order auditory fibers as a simple renewal process. They attempted to use the multimodal distribution of the IATs for low-frequency sinusoidal stimuli to distinguish between counting and timing mechanisms; the data seem to weakly support the counting model within the framework of their assumptions. As with the McGill–Goldberg work, this model is predicated on a power-law relationship between count rate and energy; a number of other special conditions are also required (Jesteadt, Wier, and Green, 1977; Wier, Jesteadt, and Green, 1977). Sanderson (1975) calculated performance bounds for a related model, based on the multimode distribution of the IATs and on neural pulse deletions. However, the results of his corrected calculation (Sanderson, 1976) are not in accord with the observed near miss to Weber's law. Following Siebert (1965, 1968), McGill (1967), and Penner (1972), we assume that the simple Poisson counting distribution provides a useful point of departure.

The model that is, perhaps, most similar to the one we analyze is that employed by Siebert (1968). He envisioned a system consisting of multiple channels and incorporated both spread of excitation and a saturating nonlinearity. As in Penner's model, the saturation is introduced prior to transduction, in such a way that the compressed stimulus undergoes Poisson transduction in a number of channels. The neural counts are added after weighting. Siebert also accounts for the experimental observation that neural counts arise from spontaneous activity, and he incorporates into his model a neural channel density that is nonuniform in frequency. As in all of his work, stimulus fluctuations are assumed to be unimportant. From a calculation of the bounds on the discrimination performance, Siebert concludes that the more central parts of the auditory system behave nearly optimally, and that Weber's Law should be obeyed at sufficiently high intensity baselines. In a subsequent study on frequency discrimination, Siebert (1970) developed a somewhat different model based on nonlinear transduction to a nonstationary Poisson process. As Jesteadt, Wier, and Green (1977, pp. 174–175) have pointed out, however, this model is in disagreement with various psychophysical data. In particular, Siebert's models (1965, 1968, 1970) do not come to grips with the observed near miss to Weber's Law for pure-tone intensity discrimination.

Our model differs from Siebert's (1968) in a number of significant respects: (1) Our detection system is assumed to be driven by the stimulus *energy*; (2) in place of an arbitrary saturating nonlinearity prior to Poisson transduction, we assume that saturation arises from refractoriness in the neural pulse train so that the resulting process is distinctly non-Poisson; (3) we assume a uniform (in frequency) neural channel density for simplicity (we find that the inclusion of a realistic density function does not appreciably affect our results); (4) we ignore noise arising from the spontaneous firing of the auditory fibers (there is some justification for this inasmuch as the presence of a stimulus appears to inhibit the generation of spontaneous neural pulses); (5) we do not confine the locus of saturation and spread of excitation exclusively to the cochlea,[4] and (6) we find that a simple *unweighted* sum of counts suffices for arriving at a decision.

In Sec. I, we deal with the detection model. This is followed by a study of pure-tone intensity discrimination in which we utilize both a refractoriness-based model and a crude saturation model (Sec. II). The latter is useful primarily as a conceptual aid and is expected to provide useful results only for high levels of the baseline intensity. In Sec. III we present results for various values of the baseline intensity and in Sec. IV we present the conclusion.

I. DETECTION MODEL

A. Qualitative description

To account for pure-tone intensity discrimination, we propose a neural-counting model that incorporates both saturation and spread-of-excitation effects. Our work draws on various contributions in the auditory literature, particularly those of McGill (1967), Siebert (1968), and Penner (1972). Following McGill (1967), we assume that the existence of phase-locked firing has little to do with intensity discrimination; we consider the underlying count n for each neural channel to be a Poisson random variable driven by the stimulus energy. We thereby disregard the role of periodicity, relying exclusively on place mechanisms; this is consistent with the conclusions reached by Siebert (1970). The information is assumed to be contained in the number of neural impulses observed on a collection of parallel channels during an unspecified, but fixed, counting interval (observation time).

Though a variety of formulas has been presented to mathematically describe the saturation of neural-counting rate with increasing stimulus intensity or energy (see, for example, Zwislocki, 1973), we use the simple rectangular hyperbola [see Eq. (7)]. We regard the saturation of counts as arising from a fixed nonparalyzable dead time following the registration of each count[1] (Parzen, 1962); indeed, the reduction of counts due to such dead-time effects leads directly and naturally to the rectangular hyperbolic function (Feller, 1948) for the relation between neural-counting rate and stimulus energy, though this rationale has not been previously considered in the audition literature. Our understanding of dead-time modified processes draws heavily on work in a variety of fields including nuclear particle counting (Parzen, 1962; Müller, 1973, 1974), optical photon counting (Cantor and Teich, 1975; Teich and McGill, 1976; Vannucci and Teich, 1978; Teich and Vannucci, 1978; Teich and Cantor, 1978), and neural counting (Ricciardi and Esposito, 1966; Teich and McGill, 1976). A similar refractoriness model has recently been used by Teich, Matin, and Cantor (1978) to describe the maintained discharge in the retinal ganglion cell of the cat. Saturation arising from refractoriness differs in character from the compressional saturation considered in other models. This is probably most easily understood in terms of the mean-to-variance ratio which, for the models used by Siebert (1968), McGill and Goldberg (1968a, 1968b), and Penner (1972), is always unity (at a given value of the stimulus energy) since the neural count is a Poisson random variable in spite of the compression. For the nonparalyzable dead-time model, on the other hand, the mean-to-variance ratio increases monotonically with the driving energy [see Eqs. (7) and (8)], representing a very different kind of process.

We consider the spread-of-excitation along the basilar membrane with increasing stimulus energy to arise from the increasing contributions of channels with characteristic frequencies far from the excitation frequency (Galambos and Davis, 1943; Kiang *et al.*, 1965; Rose *et al.*, 1971). For simplicity, we consider the transmission characteristics of each of these channels to be describable by an N-pole linear filter (Wing, 1978), although we subsequently provide some modification of this condition to allow for asymmetric response characteristics. The parameter N (which represents the number of poles) determines how steeply the skirts of the filter fall off as a function of excitation frequency (in general it is $6N$ dB/octave for an N-pole filter).

Incorporating these two effects—saturation due to refractoriness and spread of excitation due to the tuned-filter characteristics of the channel—allows us to arrive at a theoretical detection law for pure tones that is in accord with experiment: It is the near-miss to Weber's law. We achieve this while maintaining the primary response (before refractoriness modifications) linearly proportional to incident energy so that we need not make *ad hoc* assumptions involving a power law or other compressional relationship between neural-counting rate and stimulus energy. Our detector is therefore an energy detector, and has the remarkable property of leaving Weber's law intact precisely in those conditions where it is observed in human listeners. It is worth noting, perhaps, that we achieve this success by incorporating a number of specific features of the auditory system into our model. We cannot paint the listener totally out of the picture in the simple and elegant way that Hecht, Shlaer, and Pirenne were able to for visual detection in 1942 (see, however, Teich, Prucnal, and Vannucci, 1977; Prucnal and Teich, 1978; Teich *et al.*, 1979). We are rewarded, nevertheless, by the success that a closely related model affords us in dealing with the estimation of loudness and with masking, and we shall address these problems in the future. Our approach is consistent with the work of Raab and Ades (1946), Rosenzweig (1946), and with the model of Neff and his collaborators (1975) in which discrimination tasks that excite a new neural population (e.g., intensity discrimination) do not appear to be mediated by higher neural centers (see Green, 1976, pp. 91–92).

B. Quantitative description

The overall detection model is presented schematically in Fig. 1. Each horizontal channel in the figure

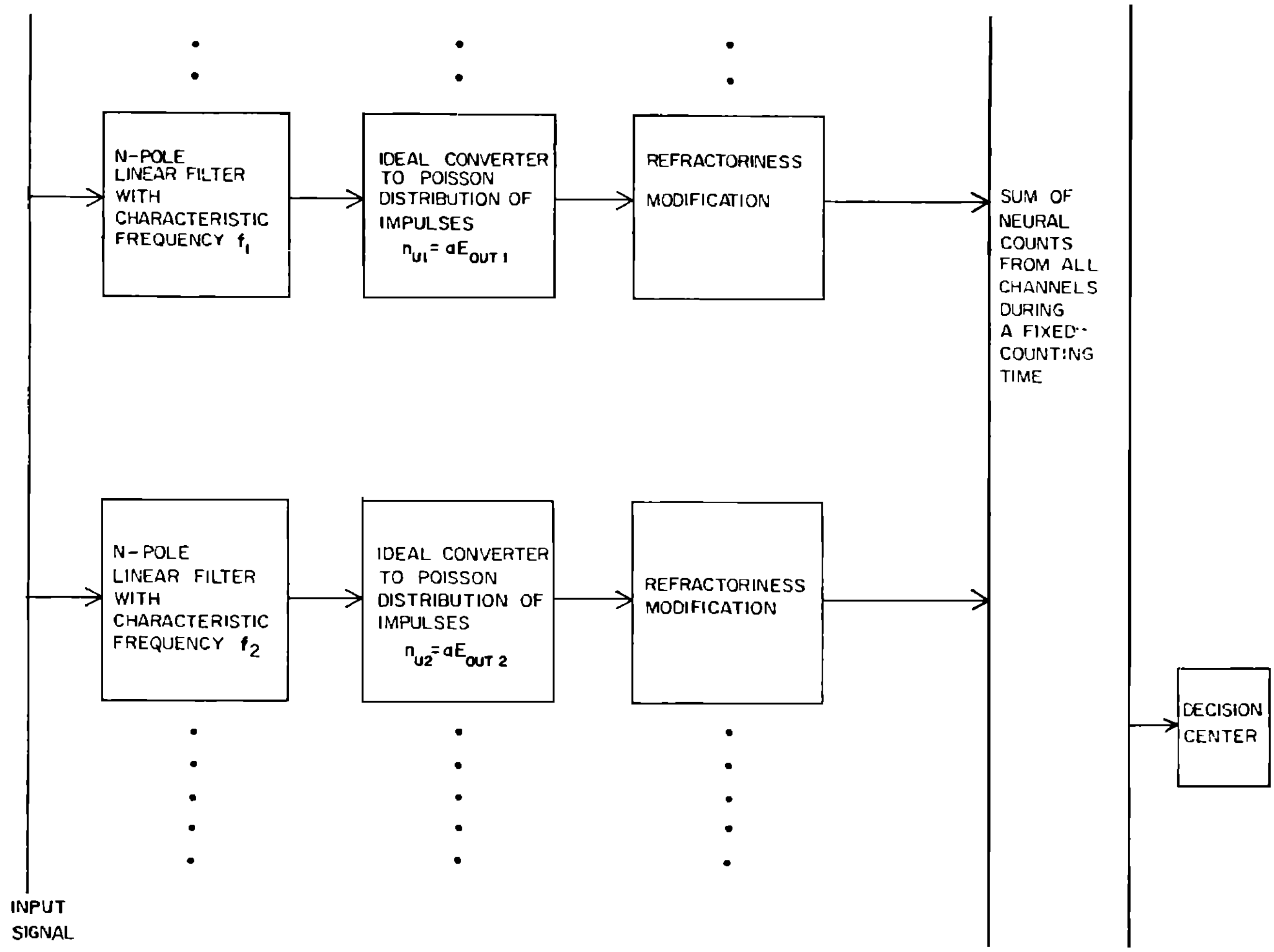

FIG. 1. Block diagram for linear filter refractoriness model (LFRM).

may represent an afferent peripheral auditory fiber (or perhaps a bundle of such fibers) and its subsequent neural path. The tuning curve characteristic of each channel (for a tone of frequency ω_T) is represented by an N-pole linear filter whose energy response is of the form (Wing, 1978)

$$E_{out}(\omega_T) = \frac{AE}{[1 + Q^2(\omega_T/\omega_0 - \omega_0/\omega_T)^2]^N}, \qquad (1)$$

where the quantities E_{out} and E represent the output and input energies, respectively, Q is the ratio of characteristic frequency to the 3-dB bandwidth for a single-pole filter, N is the number of poles, and ω_0 is the characteristic frequency of the filter. The constant A will be discussed subsequently.

We assume that all of the fibers maximally responsive to a particular frequency are included in one parallel channel while those fibers with different characteristic frequencies lie in different parallel channels. The Q parameter in Eq. (1) is not necessarily assumed to be the same for all channels.

All of the parallel channels are stimulated by the same signal but, because the characteristic frequency of each channel is different, the signal observed by each of the ideal Poisson converters will differ from one channel to another (see Fig. 1). Poisson conversion is such that the number of neural counts produced before the refractoriness modification n_{ui} is a Poisson-distributed random variable whose mean value is linearly proportional to the energy $E_{out\,i}$ that passes through the linear filter during the counting interval (the proportionality constant is designated a). The refractoriness modifications are shown as separate entries in Fig. 1 for ease of description, but they most simply will be an inherent part of the pulse-conversion mechanism.[4]

Each channel is assumed to have its own energy-to-neural pulse transducer (Johnson and Kiang, 1976). This means that the neural impulses generated in each channel are independent of those in the other channels. For nonrandom inputs, therefore

$$\sigma_T^2 = \sum_i \sigma_i^2, \qquad (2)$$

where σ_T^2 is the variance of the sum or total number of counts that reach the decision center and σ_i^2 is the variance of the count for the ith channel after refractoriness modifications have been made. The fibers and the distribution of characteristic frequencies are so dense that it will be reasonable to consider the characteristic frequencies as a continuum. Thus whenever Eq. (2) is evaluated in this paper, integration will be utilized as opposed to summation.

The nature of the decision center will depend on the physical parameter being observed. For the intensity-discrimination phenomena investigated in this paper the subject is usually asked to select which of two observed bursts is the more intense. The decision center in our model for this case determines which of the two intervals (perhaps not the same duration as the bursts) contained more neural counts. A possible alternative decision strategy (which we did not investigate) is one that selects the interval achieving a particular number of counts in the shortest time, in the manner of Luce and Green's (1972) interarrival time model.

There are various modifications that can be made to this model which will be discussed subsequently. In particular, we shall shortly see that the filter response given in Eq. (1) can be modified to nonsymmetric forms to agree more closely with the neurophysiological response functions of primary auditory fibers reported by a number of researchers (Galambos and Davis, 1943; Kiang *et al.*, 1965; Rose *et al.*, 1971).

II. PURE-TONE INTENSITY DISCRIMINATION

A. Normal approximation and detection distance

In intensity-discrimination experiments the subject is often presented with two short bursts of a pure tone at different levels. Let E_s be the energy level of the stronger tone burst and E_w the energy level of the weaker tone burst.[2] In McGill and Goldberg's (1968a, 1968b) work, the stronger level was fixed and the weaker level was adjusted until 75% correct decisions were obtained. They found experimentally that for sufficiently large E_s, a plot of $\log(E_s - E_w)$ versus $\log(E_s)$ yielded a slope of about $\frac{9}{10}$. We shall investigate the slope of the corresponding intensity-discrimination curve predicted by our linear-filter refractoriness model (LFRM).

For large levels of E_s and E_w and the case of pure tones (which are nonrandom), many independent channels are being added, so that it is reasonable to assume that the total number of counts X is a discrete random variable which is approximately normal (Gaussian). (see Parzen, 1962). Let

$$Y \triangleq X_s - X_w, \tag{3}$$

where X_s is the total number of counts when E_s is the signal energy and X_w is the total number of counts when E_w is the signal energy. Y is clearly a normal random variable (NRV) with mean $\mathrm{E}(\cdot)$ and variance σ^2 given by

$$\mathrm{E}(Y) = \mathrm{E}(X_s) - \mathrm{E}(X_w) \tag{4a}$$

and

$$\sigma^2(Y) = \sigma^2(X_s) + \sigma^2(X_w). \tag{4b}$$

We note that the Poisson convergence theorem (Çinlar, 1972; McGill, 1967, 1971) does not apply because we are dealing with multiple events from each contributing channel, as is required for dead-time effects to occur. The probability of making a correct decision as to which interval contains the larger level is equivalent to

$$P(Y>0) = 1 - \Phi[-\mathrm{E}(Y)/[\sigma^2(Y)]^{1/2}], \tag{5}$$

where $\Phi[\cdot]$ is the cumulative distribution function for NRVs. It is therefore convenient to define a detection distance h as

$$h = \frac{\mathrm{E}(Y)}{[\sigma^2(Y)]^{1/2}} = \frac{\mathrm{E}(X_s) - \mathrm{E}(X_w)}{[\sigma^2(X_s) + \sigma^2(X_w)]^{1/2}}. \tag{6}$$

In this paper we shall utilize the detection distance h given in Eq. (6); it differs from the definition of d' that is often utilized in the literature which omits the $\sigma^2(X_s)$ term in Eq. (6). The principal results however will be the same regardless of which definition of detection distance is utilized. The pure-tone intensity-discrimination results will be obtained by fixing E_s and adjusting E_w until the desired value of h is achieved. In order to accomplish this we shall require the refractoriness-modified values for $\mathrm{E}(X_s), \sigma^2(X_s), \mathrm{E}(X_w)$, and $\sigma^2(X_w)$.

B. Computation of refractoriness-modified mean and variance

The subject area of refractoriness modifications, or as the subject is known to physicists and engineers "dead-time modifications," has been under extensive investigation for many years. Most of the analyses have been conducted for conditions where modifications are small or where the unmodified counting statistics are simple Poisson. The large signal conditions that will apply to most of the results in this paper will involve substantial modifications indeed, and therefore, accurate results will be obtained only for the case of pure-tone stimuli where the underlying mechanisms obey simple Poisson statistics.

The model that will be utilized in this paper assumes that the counting system is nonparalyzable.[1] Furthermore it is assumed that the dead-time duration is a fixed (nonrandom) quantity whose numerical value can be obtained from the reciprocal of the maximum firing rate of the neural channel. This results in only a small variation from the results that would be obtained by utilizing a random dead-time duration (Parzen, 1962; Lee, 1974; Teich, Matin, and Cantor, 1978), which is likely to more closely approximate the real situation.

The refractoriness modifications for simple Poisson statistics and fixed dead time are well known. The first-order modified mean and variance are (Müller, 1974; Cantor and Teich, 1975; Teich, Matin, and Cantor, 1978)

$$\bar{n}_c = \frac{\bar{n}_u}{1 + \bar{n}_u(\tau/T)} \tag{7}$$

and

$$\sigma_c^2 = \frac{\bar{n}_u}{[1 + \bar{n}_u(\tau/T)]^3}, \tag{8}$$

where $\bar{n}_c$ is the refractoriness-modified mean, $\bar{n}_u$ is the unmodified mean, σ_c^2 is the refractoriness-modified variance, τ is the dead-time interval, and T is the counting-time interval. These modifications are effected at the output of each Poisson converter and the results are then added together (integrated in our case) to obtain the overall count mean $\bar{N}_c$ and the overall count variance Σ_c^2. For a pure tone of input energy E we have from Eq. (1) and the proportionality between $\bar{n}_u$ and E_{out},

$$\bar{n}_u = \frac{A'E}{[1 + Q^2(\omega_T/\omega_0 - \omega_0/\omega_T)^2]^N}, \tag{9}$$

where ω_T is the frequency of the tone in rad/sec, ω_0 is the characteristic frequency of the channel in rad/sec and $A'=aA$.

One finds after some minor algebra that the overall mean is

$$\overline{N}_c=\frac{A'E}{2\pi}\int_{\omega_1}^{\omega_2}\frac{d\omega_0}{[1+Q^2(\omega_T/\omega_0-\omega_0/\omega_T)^2]^N+A'E(\tau/T)}, \quad (10)$$

and that the overall variance is

$$\Sigma_c^2=\frac{A'E}{2\pi}\int_{\omega_1}^{\omega_2}\frac{[1+Q^2(\omega_T/\omega_0-\omega_0/\omega_T)^2]^{2N}\,d\omega_0}{\{[1+Q^2(\omega_T/\omega_0-\omega_0/\omega_T)^2]^N+A'E(\tau/T)\}^3}. \quad (11)$$

The limits of integration are chosen to agree with the frequency limits over which the peripheral auditory fibers are assumed to respond. In this paper $\omega_1=2\pi(50)$ and $\omega_2=2\pi(20\,000)$ are used as limits, but this choice is not critical. The factor $1/2\pi$ that appears in Eqs. (10) and (11) is equivalent to the assumption of a uniform fiber density of 1 fiber per Hz.

It should be noted that the variable of integration is the characteristic frequency of the filter and not the frequency of the incident tone which is fixed at ω_T. The maximum value of $\overline{n}_u$, and hence the maximum refractoriness modifications, occur when $\omega_0\approx\omega_T$. As ω_0 moves away from ω_T, $\overline{n}_u$ decreases as do the modifications. Eventually the modifications become small as ω_0 moves far (in the sense of octaves or decades) from ω_T. The frequency band in which the modifications are significant will be a function of the energy of the tone. The number of channels that require modification, as well as the number of channels that are significantly stimulated, will depend on the energy E. Therefore that number will be different for E_s and E_w in the pure-tone intensity-discrimination data. All of this tends to get hidden in the computations when Eqs. (10) and (11) are utilized in Eq. (6). This is particularly true because we had little success in obtaining closed-form expressions for $\overline{N}_c$ and Σ_c^2 and numerical integration was therefore utilized in the computations. In order to get a physical picture of the gross effects of refractoriness, we introduce the crude saturation model described in the next section.

C. Spread of excitation: Crude saturation model

In order to consider the effects of refractoriness in audition, we introduce a model that greatly exaggerates these effects. Let E_{af} be the energy passing through the filter and let E_m be a nonvarying saturation energy parameter such that:

(1) If $E_{af}>E_m$ then the output of the channel is nonrandom with the number of pulses per detection interval proportional to the fixed parameter E_m;

(2) If $E_{af}<E_m$ then the output of that channel is modeled as a simple Poisson process that is not affected by refractoriness.

This "rough and ready" model will be applied to situations where the input energy is much larger than E_m, and it will yield results that generally agree with those obtained from the more accurate accounting of the refractoriness effects described in the previous section. In particular, we shall find a simple analytic expression for the slope of the intensity-discrimination curve. We note that the conditions required for the crude saturation calculation are not specific to the detailed nature of the saturation (refractoriness is only one example), and the results are expected to be meaningful only for large values of the baseline intensity.

Those channels whose characteristic frequencies are near the frequency of the input signal will be completely saturated, whereas those channels whose characteristic frequencies differ considerably from that of the input tone will (in this crude model) experience no saturation effects whatever. This can be put in more quantitative form by solving the equation

$$\frac{A'E}{\{1+Q^2[\omega_T/(\omega_T+\delta)-(\omega_T+\delta)/\omega_T]^2\}^N}=E_m, \quad (12)$$

where δ is the frequency deviation from ω_T at which the upper frequency crossover from saturation to nonsaturation occurs. It is shown in the Appendix that

$$\delta\approx C_0E^{1/2N}, \quad (13)$$

where

$$C_0=\omega_TA'^{1/2N}/QE_m^{1/2N}. \quad (14)$$

Let δ_L be the frequency deviation from ω_T to the lower crossover point. For the large values of E utilized in this model, it is also shown in the Appendix that

$$\delta_L\approx\omega_T. \quad (15)$$

We can now find approximate values for the means and variances utilized in Eq. (6). In order to obtain the mean we use the assumption that $A'E_s\gg E_m$ and $A'E_w\gg E_m$. This means that nearly all of the neural counts arise from the saturated channels and we ignore the contribution of the nonsaturated tails when computing the mean. Then the expected values are

$$\mathrm{E}(X_s)\approx C_2E_m(\delta_s+\omega_T) \quad (16)$$

and

$$\mathrm{E}(X_w)\approx C_2E_m(\delta_w+\omega_T), \quad (17)$$

where C_2 is a constant and δ_s and δ_w are the upper cutoff frequencies for E_s and E_w, respectively.

The difference of these means is then obtained from Eqs. (13), (16), and (17) with the result

$$\mathrm{E}(X_s)-\mathrm{E}(X_w)\approx C_3(E_s^{1/2N}-E_w^{1/2N}), \quad (18)$$

where C_3 is the constant $C_0C_2E_m$.

Approximate values are obtained for the variances by ignoring the contributions of the saturated channels, which will be small in this case, and by considering the contribution of the upper tail [in view of Eq. (15) the lower tail does not contribute]. Since the contribution of the tail is Poisson distributed in the absence of saturation, the variance is equal to the mean and we obtain [see Eq. (10)]

$$\sigma^2(E)\approx\frac{A'E}{2\pi}\int_{\omega_T+\delta}^{\infty}\frac{d\omega_0}{[1+Q^2(\omega_T/\omega_0-\omega_0/\omega_T)^2]^N}. \quad (19)$$

We further approximate the above expression by assuming that δ is sufficiently large such that only one term in the denominator is significant, with the result

$$\sigma^2(E) \approx \frac{A' E \omega_T^{2N}}{2\pi Q^{2N}} \int_{\omega_T+\delta}^{\infty} \frac{d\omega_0}{\omega_0^{2N}}. \tag{20}$$

For very large E we have

$$\sigma^2(E) \approx C_4 E (\omega_T + \delta)^{-(2N-1)} \approx C_4 E \delta^{-(2N-1)}, \tag{21}$$

where C_4 is a constant. Then from Eqs. (13) and (21)

$$\sigma^2(E) \approx C_5 E^{1/2N}, \tag{22}$$

where again C_5 is a constant that does not depend on E.

The preceding approximations therefore result in a detection distance given approximately by

$$h \approx C \frac{E_s^{1/2N} - E_w^{1/2N}}{(E_s^{1/2N} + E_w^{1/2N})^{1/2}}, \tag{23}$$

where C is again a constant.

Let

$$\Delta E \triangleq E_s - E_w. \tag{24}$$

It has been found from the formal computations of h, using the accurate refractoriness corrections, that

$$\Delta E \ll E_s \tag{25a}$$

and

$$E_s \approx E_w. \tag{25b}$$

One now finds (as is shown in the Appendix from Eqs. (23)–(25) and the first two terms of the binomial expansion that

$$h \approx \frac{C}{2\sqrt{2}N} \frac{\Delta E}{E_s^{1-1/4N}}. \tag{26}$$

Taking the logarithm of both sides of Eq. (26) one obtains

$$\log(\Delta E) \approx \left(1 - \frac{1}{4N}\right) \log(E_s) + \log\left(\frac{2\sqrt{2}Nh}{C}\right). \tag{27}$$

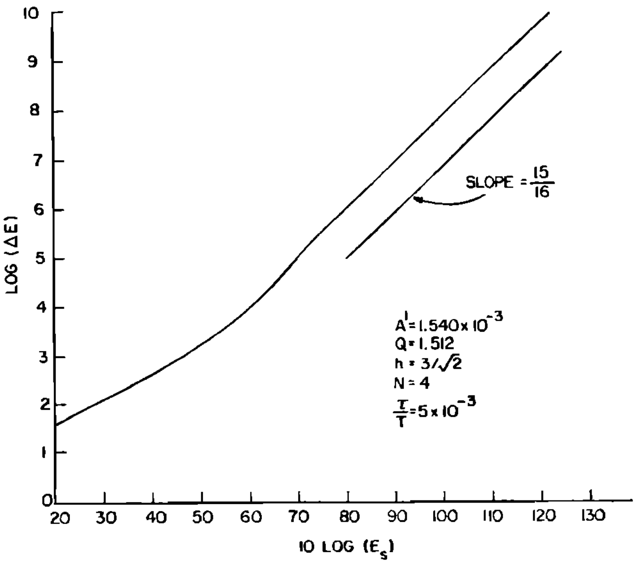

FIG. 3. Intensity-discrimination curve with $N = 4$, $h = 3/\sqrt{2}$, $Q = 1.512$, $A' = 1.540 \times 10^{-3}$, and $\tau/T = 0.005$. Also shown is a straight line of slope 15/16.

The value of h is set so that the desired error rate is achieved and therefore the last term on the right-hand side of Eq. (27) is a constant. The desired result is the slope m of the $\log(\Delta E)$ versus $\log(E_s)$ curve which, from Eq. (27), is given by

$$m = 1 - 1/4N. \tag{28}$$

In particular, when $N = 2$ the slope is $\frac{7}{8}$, when $N = 3$ the slope is $\frac{11}{12}$, and when $N = 4$ the slope is $\frac{15}{16}$. Since physically sensible values of N fall within the range $1 \leq N < \infty$, the slope of the theoretical intensity-discrimination curve will lie between $\frac{3}{4}$ and 1.

A key assumption in the preceding analysis is that $\Delta E \ll E_s$. At first glance this would seem to be in conflict with results that have been summarized by Luce and Green (1974) where it would seem that E_s is larger

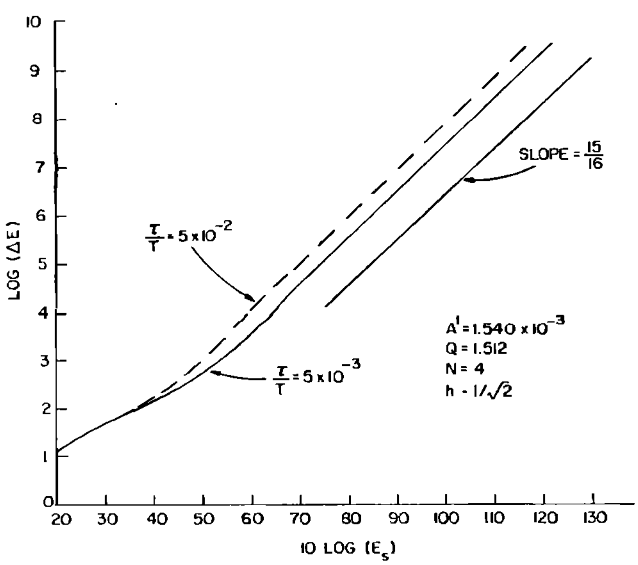

FIG. 2. Intensity-discrimination curve with $N = 4$, $h = 1/\sqrt{2}$, $Q = 1.512$, $A' = 1.540 \times 10^{-3}$, and $\tau/T = 0.005$ (solid), 0.05 (dashed). Also shown is a straight line of slope 15/16.

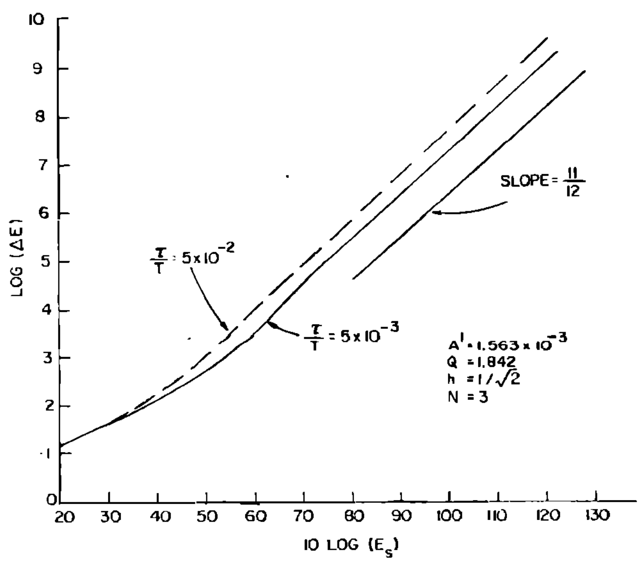

FIG. 4. Intensity-discrimination curve with $N = 3$, $h = 1/\sqrt{2}$, $Q = 1.842$, $A' = 1.563 \times 10^{-3}$, and $\tau/T = 0.005$ (solid), 0.05 (dashed). Also shown is a straight line of slope 11/12. This data is also represented in Table I.

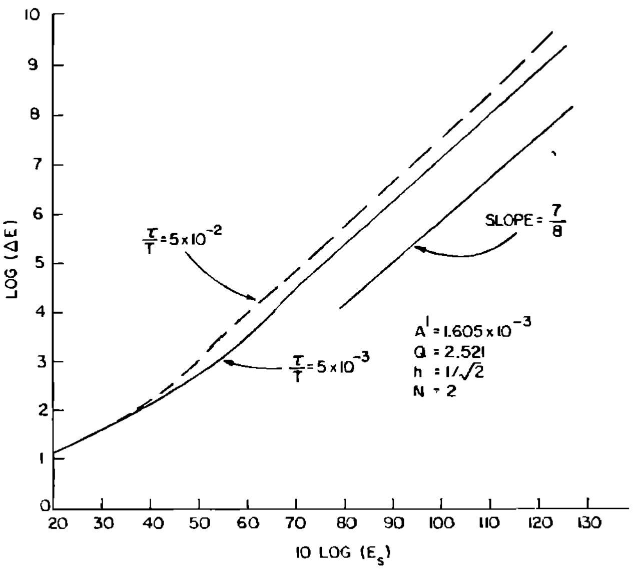

FIG. 5. Intensity-discrimination curve with $N=2$, $h=1/\sqrt{2}$, $Q=2.521$, $A'=1.605\times10^{-3}$, and $\tau/T=0.005$ (solid), 0.05 (dashed). Also shown is a straight line of slope 7/8.

than ΔE by a factor of less than 10. It should be noted however, that the data described by Luce and Green use a scale based on the sound-pressure level (SPL) whereas our data are not based on that scale. The data shown in Figs. 2–5, computed using the accurate formulas for the moments, clearly justify the assumption.

Finally, we point out that the form of the detection law for the crude saturation model specifically depends on the assumed density of neural channels (in frequency). In particular, the uniform-in-linear-frequency density implicit in the development above gives rise to the near miss to Weber's law, whereas it can be shown that a uniform-in-log-frequency density will give rise to Weber's Law. In this respect the crude saturation model and Siebert's (1968) model behave alike. The refractoriness model, on the other hand, gives rise to the near miss to Weber's law for either density.

III. RESULTS

A. Method of computation and choice of parameters

The data shown in Figs. 2–5 were computed on an IBM 370 computer by the following procedure. Specific values were selected for the constants h (the detection distance) of Eq. (6), A', N, Q, and τ/T (the dead-time ratio) of Eqs. (10) and (11). Then E_s, the energy level for the stronger burst, is run through a range of values, and for each value of E_s a value of E_w is found that satisfies Eq. (6). The integrals in Eqs. (10) and (11) were evaluated numerically and the limits ω_1 and ω_2 were chosen to correspond to a hearing range of 50 Hz–20 kHz. The frequency of the input tone was chosen to be 1 kHz in all cases.

The Q parameter was selected by setting the ratio of characteristic frequency to 10-dB bandwidth equal to 3 and then solving for Q specified in Eq. (1) (see Fig. 2). This value was arrived at from an examination of Fig. 7.6 in the monograph by Kiang *et al.* (1965) in which it appears that Q is approximately constant for characteristic frequencies below 2 kHz. The data shown in Fig. 2 are for this fixed value of Q. For comparison, we also made a computer run for the case where Kiang's 10-dB Q is set at 10.0 for all frequencies. The resulting data differed from the data shown in Fig. 2 by amounts so small that they would barely show up on a graph as a separate curve. Thus, as far as intensity discrimination is concerned, the data are relatively insensitive to the selection of the parameter Q.

Data were computed for dead-time ratios $\tau/T=0.005$ and $\tau/T=0.05$, and are presented in Figs. 2, 4, and 5. It can be seen that the slopes for large values of E_s are the same in both cases. Data were also computed for $\tau/T=0.0005$ (though not plotted in the figures) with the result again being that the final slopes would be unaltered by this change. Thus, varying the dead-time ratio provides a small shift to the straight-line portion of the curves, but the τ/T parameter does not affect the slope.

The data will also depend on the choice of parameters A' and h. The value $h=1/\sqrt{2}$ was selected so that the probability of the subject making a correct selection is 0.76 which is compatible with the 75% correct criterion often utilized in experiments. The selection of larger values for h results in larger values of ΔE for a given value of E_s. However, as can be seen from Fig. 3 (for $h=3/\sqrt{2}$) a straight line is approached asymptotically which has the same slope as that computed for $h=1/\sqrt{2}$ (see Fig. 2). The parameter A' was arbitrarily chosen so that the integral of the transfer function over the range of interest is normalized to unity. The choice of A' however will not affect the asymptotic slope of the curve as is evident from Eqs. (10) and (11). A' also incorporates the change of units implied by Eqs. (1) and (9).

The principal result of this paper, which is the slope of the intensity-discrimination curve for large values of E_s, is thus relatively independent of the choice of the above-described parameters. The number-of-poles parameter N does affect this slope, however, as can be seen from Figs. 2–5.

B. Predictions of model for large values of baseline intensity

The results shown in Figs. 2–5 demonstrate that the slopes predicted by Eq. (28) using the crude saturation model are indeed obtained when the more accurate calculations of refractoriness-modified means and variances are utilized. The slope is a function only of the number-of-poles parameter N, and in Figs. 2 and 3 a slope of $\frac{15}{16}$ is obtained when $N=4$. In Fig. 4 the slope $\frac{11}{12}$ is obtained for $N=3$, and a slope of $\frac{7}{8}$ is obtained in Fig. 5 for $N=2$. Green (1967) observed a slope of $\frac{5}{6}$ which could be obtained in our model by using $N=\frac{3}{2}$ in Eq. (1), and McGill and Goldberg (1968b) observed a slope of $\frac{9}{10}$ which could be obtained by using $N=\frac{5}{2}$. Such filters are physically possible since they are nonanticipatory, but they are not realizable by a finite number of poles. On the other hand, the slopes for the data shown in Figs. 2–5 are in excellent agreement with the data of McGill and Goldberg (1968a), Schacknow and Raab (1973), Luce and Green (1974), and Rabinowitz *et* *al.* (1976), and at the same time have the more satisfying description of an integer number of poles.

Most of the experimental data reported in the literature are represented in terms of a scale based on SPL. Our scale, on the other hand, is arbitrary because of the arbitrary choice of the parameter A'. In order to effect a direct comparison with data in the literature, the following procedure was adopted. A value for $\log(\Delta I)$ is obtained from the reported experimental data for a value of I in the vicinity of 40 dB SPL. (I and ΔI refer to intensity levels.) This is matched to $\log(\Delta E)$ in our computed data and the corresponding value of $10 \log E_s$ is then compared with I dB SPL. The $10 \log E_s$ scale is shifted by the difference between these two values. We have compared our results with the data reported by Luce and Green (1974) in this manner. The data are matched at $I = 43$ dB SPL; we find that $10 \log E_s = 63.8$ fits this point. Using this 20.8-dB difference for all larger values of E_s, we find that a good fit to Luce and Green's data is obtained for $N = 2$ (see Fig. 5).

If one examines the tuning curves of primary auditory fibers, it is readily apparent that the frequency rolloff is not symmetric. It is far steeper on the high-frequency side of the characteristic frequency. In order to examine the effects of a nonsymmetric filter characteristic, a computer run was made where the filter response was four-pole on the low side of the characteristic frequency and eight-pole on the high side. This filter response was suggested by data from the paper of Egan and Hake (1950). For the parameters utilized in Fig. 2 [only A' was changed to maintain the normalization of Eq. (1)], the nonsymmetric results were within the graphical accuracy of those obtained with a symmetric four-pole filter. The reason for this is that the change in slope only affects the response of those channels whose characteristic frequency is less than the 1 kHz utilized as the tone frequency, and these channels in turn are saturated at high signal levels.

C. Predictions of model for low and moderate values of baseline intensity

If we examine the computer data representing the predictions of our model for the lowest values of E_s, we observe that the slope has a value of about $\frac{1}{2}$. As E_s increases, the slope moves toward unity and, ultimately, settles at $\frac{11}{12} = 0.916$ for $N = 3$ (see Table I). It is remarkable that this is precisely in accord with the experimental results reported by Rabinowitz *et al.* (1976) for low and moderate values of E_s, particularly since the contribution to the count rate arising from the spontaneous discharge has been ignored and the Gaussian approximation has been used (see Parzen, 1962).

These results may be understood as follows. At the lowest level of excitation, refractoriness is absent and only one, or perhaps a small number of channels, contributes to the neural count. The counting statistics in this case are simple (unmodified) Poisson, so that the deVries–Rose law obtains, yielding a slope of $\frac{1}{2}$ for the intensity-discrimination curve. At slightly higher levels, saturation arising from refractoriness sets in, thereby driving the slope of the intensity-discrimination curve toward unity in accordance with the calculations of Bouman, Vos, and Walraven (1963). At yet higher levels, the spread of excitation yields a slope described by the near miss to Weber's law [Eq. (28) with $N = 3$] as many channels, both saturated and unsaturated, contribute to the count.

TABLE I. Computed data for pure-tone intensity discrimination with $N=3$, $h=1/\sqrt{2}$, $Q=1.842$, $A'=1.563\times10^{-3}$, and $\tau/T=0.005$. The slope is initially near $\frac{1}{2}$, moves toward 1, and finally approaches $\frac{11}{12}$. These data are also represented in Fig. 4.

$\log(E_s - E_w) = \log(\Delta E)$	$\log(E_s)$	Slope
2.00	3.70	0.511
2.27	4.20	0.525
2.55	4.70	0.567
2.88	5.20	0.665
3.29	5.70	0.821
3.76	6.20	0.945
4.25	6.70	0.975
4.73	7.20	0.960
5.20	7.70	0.944
5.67	8.20	0.933
6.13	8.70	0.927
6.60	9.20	0.923
7.06	9.70	0.921
7.52	10.20	0.920
7.97	10.70	0.919
8.43	11.20	0.918
8.89	11.70	0.918
9.35	12.20	0.918

As a caveat to the reader, we note that recent experiments performed by Jesteadt, Wier, and Green (1977) fail to provide evidence for a deviation from the near miss at low and moderate values of baseline intensity.

IV. CONCLUSION

The LFRM introduced in this paper provides a detection model that permits an initially linear dependence on the input energy and quantitatively incorporates the effects of refractoriness and spread of excitation. The predictions for pure-tone intensity discrimination are in good agreement with experimentally measured data. Corresponding results were not computed for noise-in-noise discrimination and tone-in-noise discrimination because as yet no formulas are available that yield the refractoriness corrections for these cases. The crude saturation model is used in the following, however, to show that a slope of unity is predicted for both of these cases.

The mean values for the count $E(X)$ remain proportional to $E^{1/2N}$ [see Eq. (18)]. Recall that in the crude saturation model, channels for which $E_{af} < E_m$ are treated as having no saturation corrections whatever. The variance contributed by these channels is therefore the same as that indicated by McGill (1967) and contains a dominant term proportional to the square of the nonsaturation energy; in our notation, the nonsaturation energy has the form $E^{1/2N}$ so that $(E^{1/2N})^2 = E^{1/N}$. Thus one obtains as the equivalent of Eq. (23), for both the noise-in-noise and the tone-in-noise discrimination cases,

$$h = C' \frac{E_s^{1/2N} - E_w^{1/2N}}{(E_s^{1/N} + E_w^{1/N})^{1/2}}, \tag{29}$$

where C' is a constant. Using the method outlined in the Appendix, this yields a prediction of unity slope for the intensity-discrimination curve (for sufficiently large values of E_s).

Until algorithms are developed for obtaining the refractoriness corrections for noise-in-noise and for tone-in-noise, applications of the LFRM will be constrained to nonrandom inputs. In this regard the authors have had some success in applying the model to problems in the measurement of tone loudness and masking. The results of these investigations will be reported in the near future. It has been found that whereas the use of nonsymmetric filters did not have any appreciable effect on loudness estimation, it was absolutely necessary to utilize them in studies of masking. The masking studies also showed that bandwidth limits analogous to critical bands must be incorporated into the model, whereas attempts to utilize these relatively narrow bands in intensity discrimination led to difficulties. In particular, unity slopes for the intensity-discrimination curves were obtained when the range of integration in Eqs. (10) and (11) covered only a few hundred hertz.

Another factor that could be incorporated into the LFRM is the density of neural channels (in frequency). The model presented here assumes uniform density in linear frequency though this is clearly not accurate for the peripheral auditory system (Spoendlin, 1966). It turns out, however, that a uniform-in-log-frequency assumption, as well as other realistic density functions, provides results that are substantially the same as those generated under the uniform-in-linear-frequency assumption for values of SPL within the normal hearing range. It is interesting to note that as the stimulus intensity is increased beyond the discomfort level, however, the incremental slope of the intensity discrimination curve approaches unity, as predicted by the crude saturation model. In any case, the analytical expression for the slope predicted by the crude saturation model, under the uniform-in-linear-frequency assumption, turns out to provide the proper slope for the refractoriness model, regardless of which density is employed. A more thorough discussion of the LFRM incorporating the density of neural channels will be presented elsewhere.

Finally, we point out that there are a number of other known physiological characteristics of the peripheral auditory system that we have not included in the model presented here. First, it has long been known that a pure tone generates a traveling wave with an envelope whose magnitude varies substantially with distance along the basilar membrane (Békésy, 1960). Thus the acoustic energy reaching the hair cells is nonuniformly distributed. And second, the hair-cell response itself clearly exhibits a saturating nonlinearity, as is clear from the recent experiments performed by Russell and Sellick (1978). It has been convenient to assume in this paper that saturation is associated solely with the registration of neural counts through refractoriness, or in terms of our crude saturation model. Folding in the certainty that there are other phenomena in the peripheral auditory system that we do not yet know how to properly describe, it is clear that our model is basic indeed. What is arresting is its ability to describe the outcome of psychophysical experiments such as pure-tone intensity discrimination, loudness estimation, and the masking of tones by tones, in spite of its simple nature. And it does so rather remarkably with a small number of parameters and with a locus that need not be precisely identified.

ACKNOWLEDGMENTS

This work was supported in part by the National Science Foundation and by the National Institutes of Health. We are grateful to W. J. McGill for first bringing this problem to our attention, and to E. Osman and D. M. Green for critically reading the manuscript and providing many useful suggestions.

APPENDIX: DERIVATION OF FORMULAS FOR THE CRUDE SATURATION MODEL

We rewrite Eq. (12) as

$$\frac{A'E}{E_m} = \left[1 + Q^2\left(\frac{\omega_T}{\omega_T + \delta} - \frac{\omega_T + \delta}{\omega_T}\right)^2\right]^N. \tag{A1}$$

Extracting the Nth root, we arrive at

$$\frac{(A'E/E_m)^{1/N} - 1}{Q^2} = \left(\frac{\omega_T + \delta}{\omega_T} - \frac{\omega_T}{\omega_T + \delta}\right)^2, \tag{A2}$$

which leads to

$$\left(\frac{(A'E)^{1/N} - E_m^{1/N}}{Q^2 E_m^{1/N}}\right)^{1/2} = \frac{\delta^2 + 2\omega_T \delta}{\omega_T(\omega_T + \delta)}. \tag{A3}$$

This can now be written as a quadratic equation in δ

$$\delta^2 - (B - 2)\omega_T \delta - B\omega_T^2 = 0, \tag{A4}$$

where

$$B = \left(\frac{(A'E)^{1/N} - E_m^{1/N}}{Q^2 E_m^{1/N}}\right)^{1/2}. \tag{A5}$$

The solution of Eq. (A4) is

$$\delta = (\omega_T/2)[(B-2) \pm (B^2 + 4)^{1/2}]. \tag{A6}$$

We assume that E is sufficiently large such that $A'E \gg E_m$ and that $B \gg 2$. Ignoring the negative solution for δ, we obtain

$$\delta \approx \omega_T B \approx (\omega_T/Q)(A'/E_m)^{1/2N} E^{1/2N}. \tag{A7}$$

Equations (13) and (14) follow directly from Eq. (A7).

A similar analysis can be performed to obtain the lower cutoff point. Let δ_L be the frequency deviation from ω_T and let

$$d_L = \omega_T - \delta_L. \tag{A8}$$

The equation for d_L is then

$$\frac{A'E}{E_m} = \left[1 + Q^2\left(\frac{\omega_T}{d_L} - \frac{d_L}{\omega_T}\right)^2\right]^N, \tag{A9}$$

which leads to the quadratic equation

$$d_L^2 + d_L\omega_T B - \omega_T^2 = 0. \qquad (A10)$$

The positive root of Eq. (A10) is

$$d_L = (\omega_T/2)[(B^2+4)^{1/2} - B]. \qquad (A11)$$

We note that

$$(B^2+4)^{1/2} = B(1+4/B^2)^{1/2} \approx B(1+2/B^2), \qquad (A12)$$

which leads to

$$d_L = \omega_T/B \qquad (A13a)$$

and

$$\delta_L = \omega_T(1-1/B) \approx \omega_T. \qquad (A13b)$$

This is identical to Eq. (15).

To obtain Eq. (26) from Eq. (23) we proceed as follows. From Eq. (24)

$$E_s = E_w + \Delta E \qquad (A14a)$$

and

$$E_s^{1/2N} = (E_w + \Delta E)^{1/2N}, \qquad (A14b)$$

or

$$E_s^{1/2N} = E_w^{1/2N}(1+\Delta E/E_w)^{1/2N}. \qquad (A15)$$

We retain the first two terms of the binomial expansion for the right-hand side of Eq. (A15) with the result

$$E_s^{1/2N} \approx E_w^{1/2N}[1+(1/2N)(\Delta E/E_w)]. \qquad (A16)$$

Thus

$$E_s^{1/2N} - E_w^{1/2N} \approx (1/2N)(\Delta E/E_w^{1-1/2N}). \qquad (A17)$$

In the denominator of Eq. (23) we use the relation

$$E_s^{1/2N} + E_w^{1/2N} \approx 2E_w^{1/2N}, \qquad (A18)$$

so that Eq. (26) is readily obtained from Eqs. (A17) and (A18) since $E_w \approx E_s$.

[1]We use the terms "dead time" and "refractoriness" interchangeably; see Teich, Matin, and Cantor (1978). The dead time is said to be nonparalyzable (or nonextended) when events occurring during the dead-time interval are not registered and do not extend this interval; see Müller (1973, 1974) and Libert (1975).

[2]The intensity-discrimination curve is the logarithm of the just-detectable increment (or decrement) in tone intensity (or tone energy), $\Delta E = E_s - E_w$, versus the logarithm of the intensity (or energy) of the background tone, E_s (or E_w). It is also called the masking function. To make contact with the notation used by McGill and Goldberg (1968a, 1968b), note that our E_s is their E_o, our E_w is their $E_o - E_s$, and our ΔE is their E_s.

[3]The experiments have almost surely been performed on a selected sample of fibers, however. See Spoendlin (1966) and Green (1976, p. 265).

[4]Another plausible way in which this process may occur is the following. Consider the pooled process arising from a collection of individual peripheral fibers as constituting a single (Poisson) neural channel at some higher station in the chain to the auditory cortex. In that case, the pertinent dead-time modification would occur at that higher point, rather than at the primary fiber itself, so that the intensity-discrimination mechanism would involve central as well as peripheral mechanisms. The block diagram in Fig. 1, as well as all of our calculations, clearly also apply to such a characterization.

Békésy, G. v. (1960). *Experiments in Hearing* (McGraw-Hill, New York), p. 448.

Bos, C. E., and deBoer, E. (1966). "Masking and discrimination," J. Acoust. Soc. Am. 39, 708–715.

Bouman, M. A., Vos, J., and Walraven, P. (1963). "Fluctuation theory of luminance and chromaticity discrimination," J. Opt. Soc. Am. 53, 121–128.

Campbell, R. A. (1966). "Auditory intensity perception and neural coding," J. Acoust. Soc. Am. 39, 1030–1033.

Campbell, R. A., and Lasky, E. Z. (1967). "Masker level and sinusoidal-signal detection," J. Acoust. Soc. Am. 42, 972–976.

Cantor, B. I., and Teich, M. C. (1975). "Dead-time-corrected photocounting distributions for laser radiation," J. Opt. Soc. Am. 65, 786–791.

Churcher, B. G., King, A. J., and Davies, H. (1934). "The minimum perceptible change of intensity of a pure tone," Phil. Mag. 18, 927–939.

Çinlar, E. (1972). "Superposition of point processes," in *Stochastic Point Processes: Statistical Analysis, Theory, and Applications*, edited by P. A. W. Lewis (Wiley, New York), pp. 549–606.

deVries, H. (1943). "The quantum character of light and its bearing upon threshold of vision, the differential sensitivity and acuity of the eye," Physica 10, 553–564.

Dimmick, F. L., and Olson, R. M. (1941). "The intensive difference limen in audition," J. Acoust. Soc. Am. 12, 517–525.

Egan, J. P., and Hake, H. W. (1950). "On the masking pattern of a simple auditory stimulus," J. Acoust. Soc. Am. 22, 622–630.

Feller, W. (1948). "On probability problems in the theory of counters," in *Studies and Essays: A Volume for the Anniversary of Courant* (Wiley, New York), pp. 105–115.

Galambos, R., and Davis, H. (1943). "The response of single auditory nerve fibers to acoustic stimulation," J. Neurophysiol. 6, 39–57.

Green, D. M. (1967). "Additivity of masking," J. Acoust. Soc. Am. 41, 1517–1525.

Green, D. M. (1976). *An Introduction to Hearing* (Lawrence Erlbaum Associates-Halsted-Wiley, Hillsdale, NJ).

Green, D. M., Nachmias, J., Kearney, J. K., and Jeffress, L. A. (1979). "Intensity discrimination with gated and continuous sinusoids," J. Acoust. Soc. Am. 66, 1051–1056.

Harris, J. D. (1963). "Loudness discrimination," J. Speech Hear. Disord., Mono. Suppl. #11, pp. 1–63.

Hawkins, J. E., Jr., and Stevens, S. S. (1950). "The masking of pure tones and of speech by white noise," J. Acoust. Soc. Am. 22, 6–13.

Hecht, S., Shlaer, S., and Pirenne, M. H. (1942). "Energy, quanta and vision," J. Gen. Physiol. 25, 819–840.

Jesteadt, W., Wier, C. C., and Green, D. M. (1977). "Intensity discrimination as a function of frequency and sensation level," J. Acoust. Soc. Am. 61, 169–177.

Johnson, D. H., and Kiang, N. Y. S. (1976). "Analysis of discharges recorded simultaneously from pairs of auditory nerve fibers," Biophys. J. 16, 719–734.

Kiang, N. Y.S., Watanabe, T., Thomas, E. C., and Clark, L. F. (1965). *Discharge Patterns of Single Fibers in the Cat's Auditory Nerve*, Research Monograph No. 35 (MIT Cambridge, MA).

Lee, P. A. (1974). "Output response of non-linear switching element with stochastic dead time," Kybernetik 15, 187–191.

Libert, J. (1975). "Statistique de comptage: à propos d'une expérience récente," Nucl. Instrum. Methods 126, 589–590.

Luce, R. D., and Green, D. M. (1972). "A neural timing theory for response times and the psychophysics of intensity," Psychol. Rev. 79, 14–57.

Luce, R. D., and Green, D. M. (1974). "Neural coding and

psychophysical discrimination data," J. Acoust. Soc. Am. 56, 1554–1564.
Luce, R. D., and Green, D. M. (1975). "Erratum: Neural coding and psychophysical discrimination," J. Acoust. Soc. Am. 57, 1552.
McGill, W. J. (1967). "Neural counting mechanisms and energy detection in audition," J. Math. Psychol. 4, 351–376.
McGill, W. J. (1971). "Poisson counting and detection in sensory systems," in *Concepts of Communication: Interpersonal, Intrapersonal, and Mathematical*, edited by E. F. Beckenbach and C. B. Tompkins (Wiley, New York), pp. 257–281.
McGill, W. J., and Goldberg, J. P. (1968a). "Pure-tone intensity discrimination and energy detection," J. Acoust. Soc. Am. 44, 576–581.
McGill, W. J., and Goldberg, J. P. (1968b). "A study of the near-miss involving Weber's law and pure-tone intensity discrimination," Percept. Psychophys. 4, 105–109.
Miller, G. A. (1947). "Sensitivity to changes in the intensity of white noise and its relation to masking and loudness," J. Acoust. Soc. Am. 19, 609–619.
Moore, B. C. J., and Raab, D. H. (1974). "Pure-tone intensity discrimination: Some experiments relating to the near-miss to Weber's law," J. Acoust. Soc. Am. 55, 1049–1054.
Müller, J. W. (1973). "Dead-time problems," Nucl. Instrum. Methods 112, 47–57.
Müller, J. W. (1974). "Some formulae for a dead-time-distorted Poisson process," Nucl. Instrum. Methods 117, 401–404.
Neff, W. D., Diamond, I. T., and Casseday, J. H. (1975). "Behavioral Studies of auditory discrimination: Central Nervous System," in *Handbook of Sensory Physiology, Auditory System*, edited by W. D. Keidel and W. D. Neff (Springer-Verlag, Berlin), Vol. V/2, pp. 307–400.
Parzen, E. (1962). *Stochastic Processes* (Holden-Day, San Francisco), pp. 117–186.
Penner, M. J. (1972). "Neural or energy summation in a Poisson counting model," J. Math. Psychol. 9, 286–293.
Penner, M. J., Leshowitz, B., Cudahy, E., and Ricard, G. (1974). "Intensity discrimination for pulsed sinusoids of various frequencies," Percept. Psychophys. 15, 568–570.
Prucnal, P. R., and Teich, M. C. (1978). "Single-threshold detection of a random signal in noise with multiple independent observations: 1. Discrete case with application to optical communications," Appl. Opt. 17, 3576–3583.
Raab, D. H., and Ades, H. W. (1946). "Cortical and mid-brain mediation of a conditioned discrimination of acoustic intensities," Am. J. Psychol. 59, 59–83.
Rabinowitz, W. M., Lim, J. S., Braida, L. D., and Durlach, N. I. (1976). "Intensity perception. VI. Summary of recent data on deviations from Weber's law for 1000-Hz tone pulses," J. Acoust. Soc. Am. 59, 1506–1509.
Ricciardi, L. M., and Esposito, F. (1966). "On some distribution functions for non-linear switching elements with finite dead time," Kybernetik 3, 148–152.
Riesz, R. R. (1928). "Differential sensitivity of the ear for pure tones," Phys. Rev. 31, 867–875.
Rose, A. (1942). "The relative sensitivities of television pickup tubes, photographic film, and the human eye," Proc. IRE 30, 293–300.
Rose, J. E., Hind, J. E., Anderson, D. J., and Brugge, J. F. (1971). "Some effects of stimulus intensity on response of auditory nerve fibers in the squirrel monkey," J. Neurophysiol. 34, 685–699.
Rosenzweig, M. (1946). "Discrimination of auditory intensities in the cat," Am. J. Psychol. 59, 127–136.
Russell, I. J., and Sellick, P. M. (1978). "Intracellular studies of hair cells in the mammalian cochlea," J. Physiol. (London) 284, 261–290.
Sanderson, A. C. (1975). "Discrimination of neural coding parameters in the auditory system," IEEE Trans. Syst., Man, Cyber. SMC-5, 533–542.
Sanderson, A. C. (1976). "Comments on the paper 'Discrimination of neural coding parameters in the auditory system'" (unpublished).
Schacknow, P. N., and Raab, D. H. (1973). "Intensity discrimination of tone bursts and the form of the Weber function," Percept. Psychophys. 14, 449–450.
Schuknecht, H. F. (1960). "Neuroanatomical correlates of auditory sensitivity and pitch discrimination in the cat," in *Neural Mechanisms of the Auditory and Vestibular Systems*, edited by G. L. Rasmussen and W. F. Windle (Thomas, Springfield, IL).
Siebert, W. M. (1965). "Some implications of the stochastic behavior of primary auditory neurons," Kybernetik 2, 206–215.
Siebert, W. M. (1968). "Stimulus transformations in the peripheral auditory system," in *Recognizing Patterns*, edited by P. A. Kolers and M. Eden (MIT, Cambridge, MA), pp. 104–133.
Siebert, W. M. (1970). "Frequency discrimination in the auditory system: Place or periodicity mechanisms?" Proc. IEEE 58, 723–730.
Spoendlin, H. (1966). "The organization of the cochlear receptor," *Advances in Oto-Rhino-Laryngology* (Karger, New York), Vol. 13.
Teich, M. C., and Cantor, B. I. (1978). "Information, error, and imaging in deadtime-perturbed doubly stochastic Poisson counting systems," IEEE J. Quant. Electron. QE-14, 993–1003.
Teich, M. C., Matin, L., and Cantor, B. I. (1978). "Refractoriness in the maintained discharge of the cat's retinal ganglion cell," J. Opt. Soc. Am. 68, 386–402.
Teich, M. C., and McGill, W. J. (1976). "Neural counting and photon counting in the presence of dead time," Phys. Rev. Lett. 36, 754–758, 1473.
Teich, M. C., Prucnal, P. R., and Vannucci, G. (1977). "Optimum photon detection with a simple counting processor," Opt. Lett. 1, 208–210.
Teich, M. C., Prucnal, P. R., Vannucci, G., Breton, M. E., and McGill, W. J. (1979). "Role of quantum fluctuations and the Neyman type—A distribution in human vision," J. Opt. Soc. Am. 69, 1469.
Teich, M. C., and Vannucci, G. (1978). "Observation of dead-time-modified photocounting distributions for modulated laser radiation," J. Opt. Soc. Am. 68, 1338–1342.
Vannucci, G., and Teich, M.C. (1978). "Effects of rate variation on the counting statistics of dead-time-modified Poisson processes," Opt. Commun. 25, 267–272.
Viemeister, N. F. (1972). "Intensity discrimination of pulsed sinusoids: The effects of filtered noise," J. Acoust. Soc. Am. 51, 1265–1269.
Whitfield, I. C. (1967). *The Auditory Pathway* (Arnold, London).
Wier, C. C., Jesteadt, W., and Green, D. M. (1977). "Frequency discrimination as a function of frequency and sensation level," J. Acoust. Soc. Am. 61, 178–184.
Wing, O. (1978). *Circuit Theory with Computer Methods* (McGraw-Hill, 1978), p. 366.
Zwicker, E. (1956). "Die elementaren Grundlagen zur Bestimmung der Informationskapazität des Gehörs," Acustica 6, 365–381.
Zwicker, E. (1970). "Masking and psychological excitation as consequences of the ear's frequency analysis," in *Frequency Analysis and Periodicity Detection in Hearing*, edited by R. Plomp and G. F. Smoorenburg (Sijthoff, Leiden), pp. 376–396.
Zwislocki, J. J. (1973). "On intensity characteristics of sensory receptors: A generalized function," Kybernetik 12, 169–183.